catalysts

MDPI

Article

Response Surface Methodology for Optimization of Bisphenol A Degradation Using Fe_3O_4-Activated Persulfate

Shufang Chen * and Yan Yu

School of Energy and Environmental Engineering, Jilin University of Architecture and Technology, Changchun 130114, China
* Correspondence: chenshufang1262022@126.com

Abstract: In this study, the degradation of bisphenol A (BPA) by a magnetite (Fe_3O_4)/persulfate (PS) system was investigated. The effects of magnetite dosage, PS concentration, BPA concentration, and pH on Fe_3O_4-activated PS in degrading BPA were investigated using single factor experiments. magnetite dosage, PS concentration, and pH were identified as factors in the response surface experimental protocol. Using Box-Behnken analysis, a quadratic model with a high correlation coefficient (0.9152) was obtained, which was accurate in predicting the experimental results. The optimal parameter conditions obtained by the response surface methodology (RSM) were [magnetite] = 0.3 g/L, [PS] = 0.26 mM, and pH = 4.9, under which the predicted BPA degradation rate was 59.54%, close to the real value.

Keywords: bisphenol A; persulfate; response surface methodology; magnetite

check for updates

Citation: Chen, S.; Yu, Y. Response Surface Methodology for Optimization of Bisphenol A Degradation Using Fe_3O_4-Activated Persulfate. *Catalysts* **2023**, *13*, 128. https://doi.org/10.3390/catal13010128

Academic Editor: Wenhui Wang

Received: 22 November 2022
Revised: 27 December 2022
Accepted: 3 January 2023
Published: 6 January 2023

1. Introduction

In recent years, the extensive industrial usage of bisphenol A (BPA) and unregulated discharge of wastewater have led to widespread residues of BPA in surface water sources. According to previous study, trace amounts of BPA in water sources can interfere with the endocrine system of organisms and the humans [1]. Current studies on BPA have mostly focused on its origin, migration transformation, and potential endocrine disruption to organisms in the natural water environment. BPA is a diphenylmethane derivative with two hydroxyphenyl groups (Table 1) [2], and it is very difficult to be biodegraded in natural water bodies. As conventional water treatment processes (coagulation, sedimentation, filtration, etc.) have a limited effect on BPA degradation [3], it is necessary to develop new processes to treat endocrine disruptors (including BPA) in water sources.

The effectiveness of advanced oxidation processes (AOPs) for the degradation of refractory pollutants such as BPA in water is generally recognized. The AOPs mainly rely on the strong oxidizing free radicals (hydroxyl radicals, •OH and sulfate radicals, $SO_4^{\bullet-}$) generated in the water to degrade organic pollutants. Hydrogen peroxide (H_2O_2) and ozone (O_3) can be activated to produce hydroxyl radicals in several AOPs, such as UV/H_2O_2, UV/O_3, H_2O_2/O_3, UV/photocatalyst, Fenton (Fe^{2+}/H_2O_2), Fenton-like processes, and various combinations of these [4,5]. These processes have been studied earlier, and especially the Fenton and ozone processes have already been applied in actual wastewater treatment. However, these processes still have the disadvantages of poor stability of the oxidizing agent and harsh reaction conditions [4]. Currently, AOPs based on sulfate radicals have attracted a lot of attention in the treatment of refractory pollutants, even BPA [6,7], as sulfate radicals are considered to be more advantageous than hydroxyl radicals in oxidizing organic matter. The sulfate radicals (E_0 = 2.6–3.1 V) possess a higher redox potential than the hydroxyl radicals (E_0 = 1.9–2.8 V) [8], and the half-life of the sulfate radicals ($t_{1/2}$ = 30–40 μs) is longer than that of the hydroxyl radicals ($t_{1/2} \leq 1$ μs) [9]. Due to the higher selectivity of sulfate radicals compared to hydroxyl radicals, sulfate radicals

can be employed to attack directly at specific functional groups (–NH_2,–OH, and –OR) via electron transfer reactions [9,10].

Table 1. Properties of BPA.

Name	CAS No.	Molecular Formula	Molecular Weight	Color	Structure
Bisphenol A	80-05-7	$C_{15}H_{16}O_2$	228.29	White	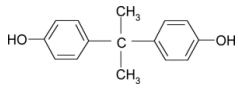

Previous studies have shown that sulfate radicals generated from peroxymonosulfate (PMS, HSO_5^-) or persulfate (PS, $S_2O_8^{2-}$) can effectively degrade refractory pollutants in wastewater under the action of carbon-based materials, transition metals (Fe, Co, Cu, Mn), ultraviolet light, microwaves, and ultrasound [11–16]. PMS or PS is a monosubstituted or symmetrically substituted derivative of hydrogen peroxide by sulfo moiety [17]. PMS possesses an asymmetrical structure the distance of the O-O bond is 1.453 Å, and the bond energy is estimated to be 140–213.3 kJ/mol [12]. PS has a symmetrical structure; the distance of the O-O bond is 1.497 Å, and it has a bond energy of 140 kJ/mol [12]. Sodium persulfate with high stability and water solubility is preferred for use in wastewater treatment [17]. According to the previous report, the transition metal Fe has been extensively studied in activating PS to generate sulfate radicals to degrade refractory pollutants owing to its environmental friendliness, low price, and excellent activation of Fe [18]. Zero-valent iron and ferrous salt were used in the studies of activating PS to degrade BPA, and the influence of some reaction parameters and the reaction mechanism were clarified [19–23]. Several studies were found involving the activation of PS degradation of BPA by Fe_3O_4 (magnetite) [24–27]. Magnetite has more advantages than zero-valent iron and ferrous salt in activating PS. Since the solubility of ferrous metal is high, the ferrous iron in the solution is easy to be excessive, and the excessive ferrous iron will extinguish the sulfate radicals formed in the reaction and reduce the reaction rate [28]. While acting as a heterogeneous activator, magnetite, which contains ferrous and ferric iron, can continuously release iron into the aqueous solution, thus avoiding the problem of iron excess [29]. In addition, the equilibrium of ferrous iron and ferric iron in water can be achieved in the Fe_3O_4/PS system so that the reaction is in a stable state. Compared with the heterogeneous activator, zero-valent iron, the advantage of magnetite is that it has strong paramagnetism and can be separated under the action of an external magnetic field in solution [30]. Therefore, magnetite is considered a suitable PS catalyst for practical applications. But the current research on Fe_3O_4/PS is not enough to support its large-scale practical application in the future. Further research is especially needed in the optimization of experimental influencing factors in the Fe_3O_4/PS system towards BPA degradation.

In this paper, research on the activation of PS to degrade BPA via magnetite was carried out. Single factor experiments were performed to identify the key influencing factors in the Fe_3O_4/PS/BPA system, and the Box-Behnken response surface methodology (RSM) was used to investigate the optimal effects of the above key influencing factors on BPA degradation. This study is expected to provide a corresponding theoretical basis for the removal of endocrine disruptors, even BPA, from the Fe_3O_4/PS system.

2. Results and Discussion

2.1. Single-Factor Experiments

The effects of the dosage of magnetite, the concentration of PS, the concentration of BPA, and the initial pH on the BPA decomposition in the Fe_3O_4/PS system were investigated. The value range of each parameter was set as follows: magnetite dosage: 0, 0.1, 0.2, 0.3, 0.4, and 0.5 g/L; PS concentration: 0, 0.1, 0.2, 0.3, 0.4, and 0.5 mM; BPA concentration: 1, 2, 3, 4, and 5 mg/L; pH: 3.0, 5.0, 7.0, and 9.0.

Figure 1 shows the trend of BPA removal over time due to variations in Fe_3O_4 dosage. When the magnetite dosages were 0, 0.1, 0.2, 0.3, 0.4, and 0.5 mg/L, the corresponding BPA degradation rates at 60 min were 19.68%, 41.94%, 56.46%, 53.92%, 59.60%, and 50.96%, respectively. It can be seen that in the range of 0.2–0.5 mg/L magnetite, above 50% of BPA degradation rates were reached. Strangely, the degradation rate of 0.5 mg/L magnetite on BPA was lower than that of 0.4 mg/L magnetite. It is speculated that the reason may be the decrease in free radical concentration caused by excess Fe^{2+} from magnetite, which in turn affects the degradation of BPA. Previous studies have also found that too high a Fe_3O_4 concentration is not conducive to the degradation of target pollutants [31]. Therefore, in the subsequent RSM optimization experiments, the catalyst magnetite level can be selected around 0.4 g/L.

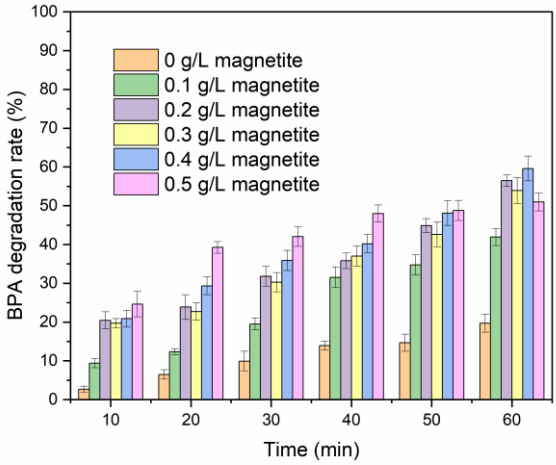

Figure 1. The effect of magnetite dosage on BPA degradation. [BPA] = 5 mg/L, [PS] = 0.2 mM, T = 20 °C, pH = 7.0.

Figure 2 depicts the effect of PS concentration variation on the BPA removal rate. When the PS was between 0.3 mM and 0.5 mM, the BPA removal rate varied between 60.62–66.56%, and this variation was not significant. Therefore, it is wasteful to inject too much oxidant. In addition, too high a PS could deplete the free radicals already generated by the reaction [32,33]. In the subsequent RSM experiments, three PS levels of 0.1 mM, 0.2 mM, and 0.3 mM were chosen.

Figure 3 shows that as the BPA concentration increased from 1.0 mg/L to 5.0 mg/L, the 60-min degradation rate of BPA decreased. It was possible that the substrate was raised but the amount of oxidant and catalyst did not change, so there were not enough free radicals available. Generally, by controlling the ratio of catalyst and oxidant and increasing their absolute amounts, the increase in initial BPA concentration can be effectively dealt with. Therefore, BPA was not selected as a parameter for the subsequent RSM experiments.

Figure 4 reveals the effect of pH value on the degradation of BPA in the Fe_3O_4/PS system. It can be seen from Figure 4 that significant BPA removals (42.22–59.16%) were achieved at pH 3.0–7.0, while the removal rate was minimal (25.50%) at pH 9.0. The reason for the better degradation effect of BPA under acidic conditions may be that magnetite can release more soluble iron ions under acid corrosion to promote the activation reaction of PS. However, under alkaline conditions, iron ions easily exist in the form of $Fe(OH)_3$, thus weakening the catalytic effect on PS. According to the data from above, three pH levels of 3.0, 5.0, and 7.0 were chosen for the RSM experiments.

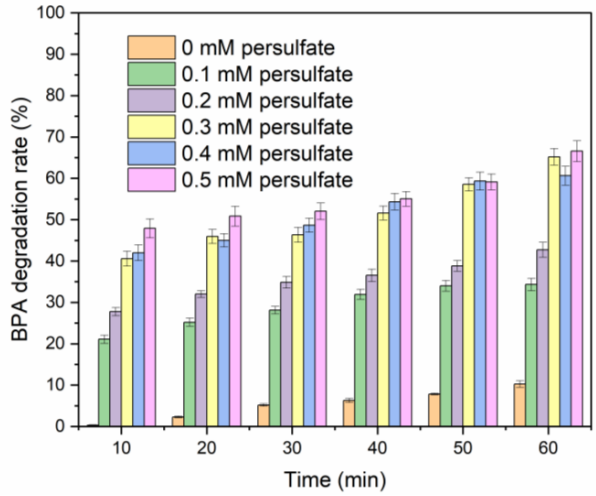

Figure 2. The effect of PS concentration on BPA degradation. [BPA] = 5 mg/L, [magnetite] = 0.1 g/L, T = 20 °C, pH = 7.0.

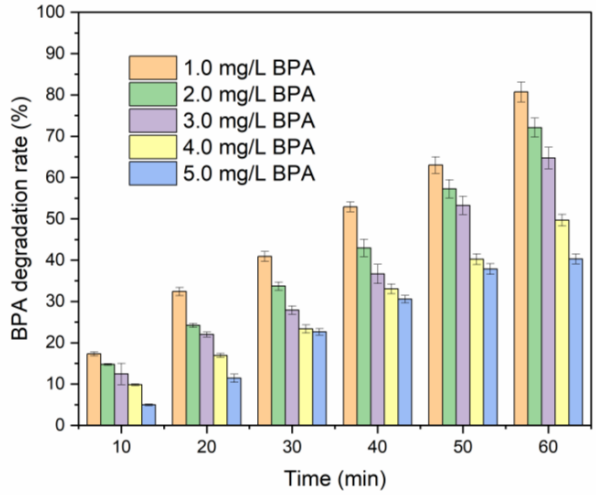

Figure 3. The effect of initial BPA concentration on BPA degradation. [PS] = 0.2 mM, [magnetite] = 0.1 g/L, T = 20 °C, pH = 7.0.

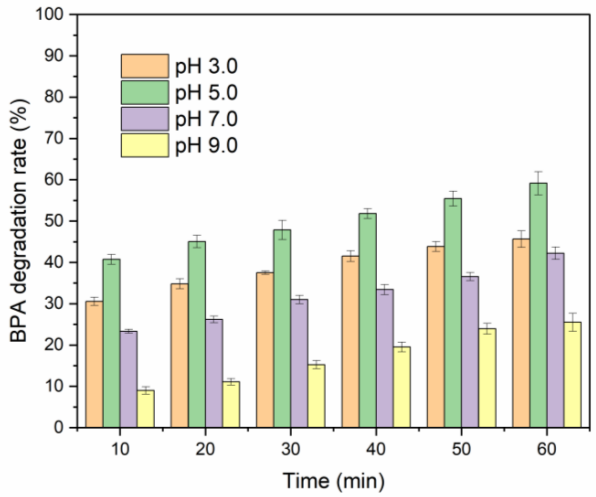

Figure 4. The effect of solution pH on BPA degradation. [BPA] = 5 mg/L, [PS] = 0.2 mM, [magnetite] = 0.1 g/L, T = 20 °C.

2.2. RSM Experiments

The magnetite dosage (A), PS concentration (B), and pH (C) were used as independent variables, and three levels were selected for each independent variable based on the results of single-factor experiments. The factor levels and codes are shown in Table 2. The Box-Behnken central combination design in Design-Expert was used to determine the experimental design scheme for the degradation of BPA by PS activated by Fe_3O_4, and the results of the experiments conducted according to the experimental scheme are shown in Table 3.

Table 2. Factors and levels of independent variables.

Independent Variables	Symbols	Range and Levels		
		−1	**0**	**+1**
Magnetite dosage (g/L)	A	0.3	0.4	0.5
PS concentration (mM)	B	0.1	0.2	0.3
Initial pH	C	3.0	5.0	7.0

Table 3. Scheme and experimental results of response surface design.

Run	A: Magnetite(g/L)	B: PS(mM)	C: Initial pH	BPA Removal (%)	
				Actual Value	Predicted Value
1	0	1	−1	16.14	25.46
2	0	−1	1	3.24	−6.08
3	0	−1	−1	9.16	9.36
4	0	0	0	50.20	52.34
5	−1	0	1	14.12	22.23
6	−1	0	−1	30.04	28.64
7	−1	1	0	65.52	57.60
8	0	0	0	59.80	52.34
9	0	0	0	46.90	52.34
10	−1	−1	0	32.48	33.69
11	1	0	−1	39.02	30.91
12	1	1	0	50.60	49.39
13	0	0	0	51.90	52.34
14	1	−1	0	26.80	34.72
15	1	0	1	11.38	12.79
16	0	1	1	16.58	16.38
17	0	0	0	52.90	52.34

Multiple regression analysis was applied to the responses and the design matrix, and the quadratic polynomial fitting equations were eestablished for magnetite dosage (A), PS concentration (B), pH (C), and BPA removal rate (Y), as shown in Equation (1).

$$Y = 52.34 - 1.79A + 9.64B - 6.13C - 2.31AB - 2.93AC + 1.59BC + 1.94A^2 - 10.42B^2 - 30.63C^2 \quad (1)$$

Table 4 illustrates the ANOVA (analysis of variance) of the regression model. The F-value of the quadratic model was 8.39, and the p-value (0.0052) was less than 0.05. A p-value < 0.05 expresses that the model is significant, while a value > 0.1000 specifies that the model is not significant [34]. The R^2 value was 0.9152. These results clearly demonstrated the stability and significance of proposed model. The adequacy of the model test is a key analytical step to verify the result is accurate or misleading [35]. Figure 5 shows that the normal plot of residuals met the straight line, suggesting that it was a normal distribution. The graph of residuals versus predicted data indicated that the residues were distributed randomly (Figure 6), attesting that the primitive observation variation was quite stable for all response results [36]. Figure 7 indicates that the predicted and actual experimental values were distributed along the linear function, indicating a significant

correlation in these values [37]. In addition, the predicted values of BPA degradation can be found in Table 3.

Table 4. ANOVA and test of significance.

Source	Sum of Squares	DF	Mean Square	F-Value	*p*-Value	
Model	5700.29	9	633.37	8.39	0.0052	significant
A-Magnetite	25.78	1	25.78	0.34	0.5773	
B-Persulfate	744.21	1	744.21	9.86	0.0164	
C-pH	300.62	1	300.62	3.98	0.0862	
AB	21.34	1	21.34	0.28	0.6113	
AC	34.34	1	34.34	0.45	0.5216	
BC	10.11	1	10.11	0.13	0.7252	
A^2	15.77	1	15.77	0.21	0.6615	
B^2	457.60	1	457.60	6.06	0.0433	
C^2	3951.59	1	3951.59	52.35	0.0002	
Residual	528.35	7	75.48			
Lack of Fit	438.02	3	146.01	6.47	0.0516	not significant
Pure Error	90.33	4				
Cor Total	6228.64	16	22.58			
R^2 = 0.9152						
Adjusted R^2 = 0.8061						
C.V.% = 25.61						

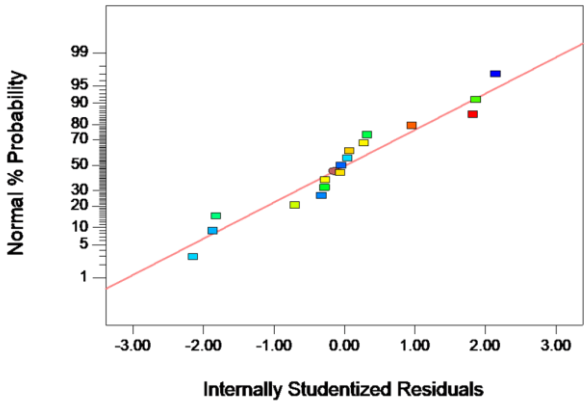

Figure 5. Normal distribution plot of residuals.

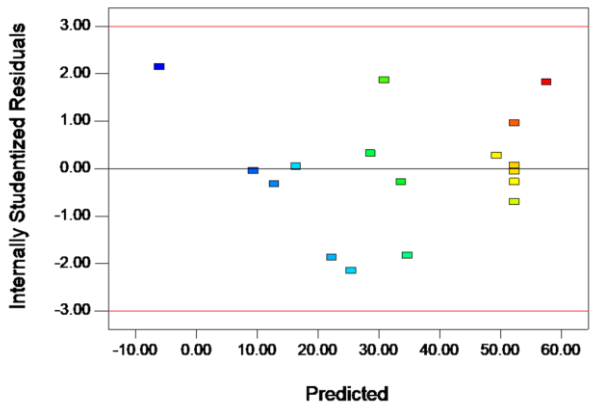

Figure 6. Residuals vs. predicted values.

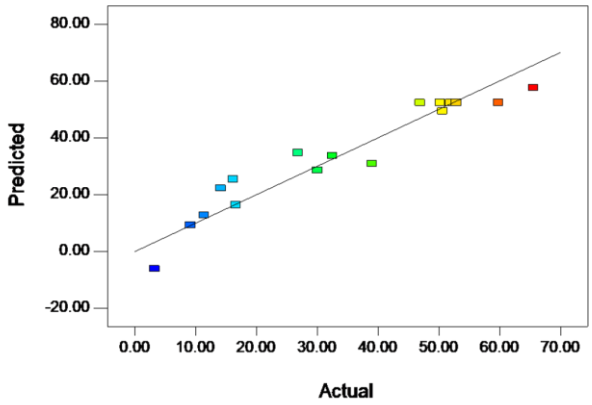

Figure 7. Actual values vs. predicted values.

The 3D response surface and contour plots are given in Figures 8–10. The nonlinear nature of the presented 3D surfaces and contour plots clearly shows considerable interactions among the studied process parameters [36]. Figure 8 showed that the change in magnetite dosage did not significantly affect the height of the surface, which meant that magnetite dosage had little effect on BPA degradation. In Figure 9, the variation in pH value caused the deformation of the curved surface more than the variation in PS concentration, indicating that the effect of pH on the degradation of BPA was greater than that of PS. As can be seen in Figure 10, the effect of pH on BPA degradation was significantly higher than that of magnetite dosage. Therefore, the factors affecting the degradation of BPA are as follows, according to their importance: pH, persulfate concentration, and magnetite dosage.

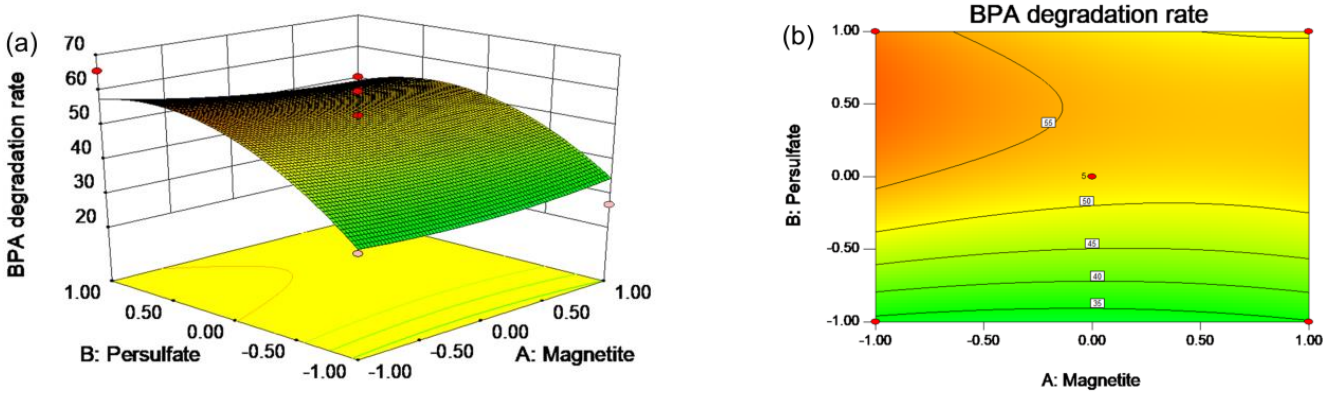

Figure 8. Response surface plot of PS and magnetite on BPA removal. (**a**) Three-dimensional plot; (**b**) Two-dimensional plot. [BPA] = 5 mg/L, [magnetite] = 0.1 g/L, pH = 5.0, T = 20 °C.

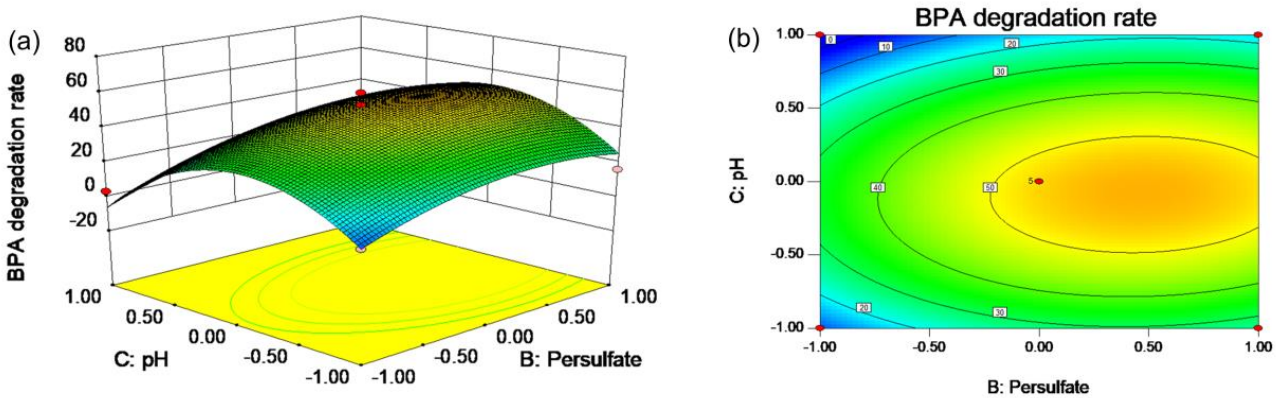

Figure 9. Response surface plot of pH and PS on BPA removal. (**a**) Three-dimensional plot; (**b**) Two-dimensional plot. [BPA] = 5 mg/L, [magnetite] = 0.4 g/L, T = 20 °C.

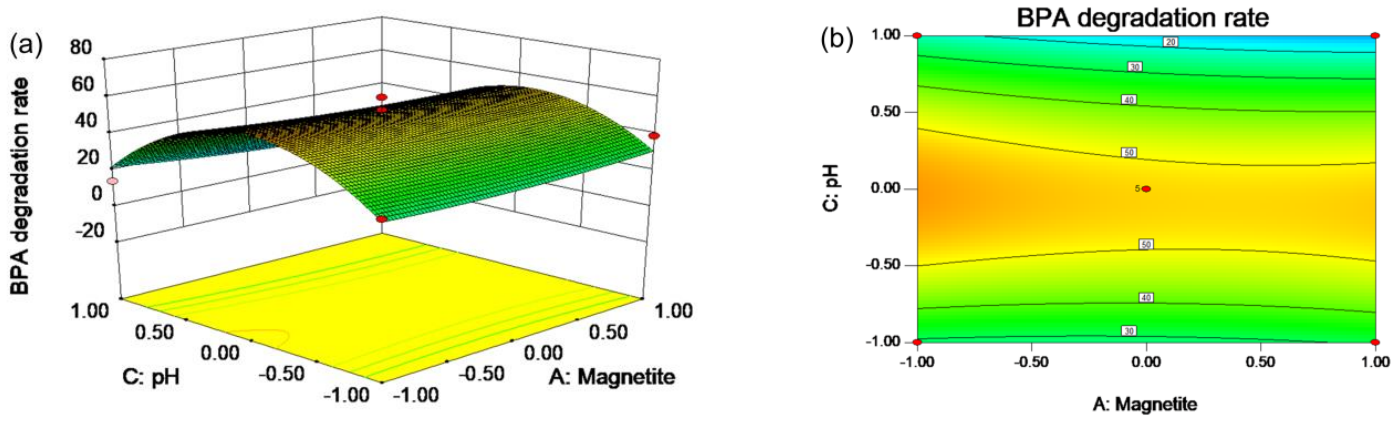

Figure 10. Response surface plot of pH and magnetite on BPA removal. (**a**) Three-dimensional plot; (**b**) Two-dimensional plot. [BPA] = 5 mg/L, [PS] = 0.2 mM, T =20 °C.

Figure 11 shows the prediction plot of optimized conditions for BPA degradation. The optimal reaction conditions obtained from the software analysis were: 0.3 g/L of magnetite, 0.26 mM of PS, and pH 4.9. The predicted BPA degradation under optimal conditions was 59.54%. The actual BPA degradation rate was 65.52% (0.3 g/L of magnetite, 0.3 mM of PS, pH 5.0). This indicated that the optimal reaction conditions were more reliable.

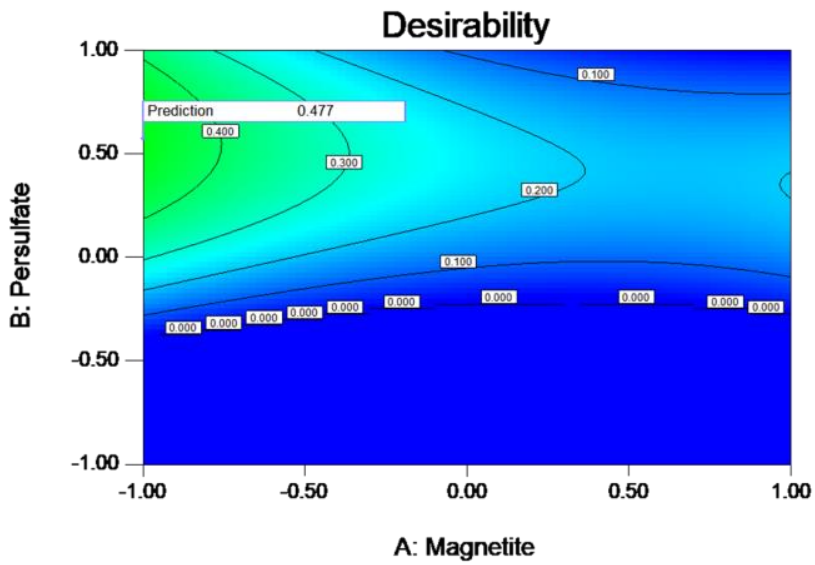

Figure 11. Optimization of experimental conditions.

3. Materials and Methods

3.1. Chemicals

Sodium persulfate ($Na_2S_2O_8$), bisphenol A ($C_{15}H_{16}O_2$), and magnetite (Fe_3O_4, its shape and size is shown in Figure 12.) were purchased from Macklin (Shanghai, China). Methanol was obtained from Nuoershi (Chengdu, China). Ultrapure water was utilized in preparing water solutions with BPA.

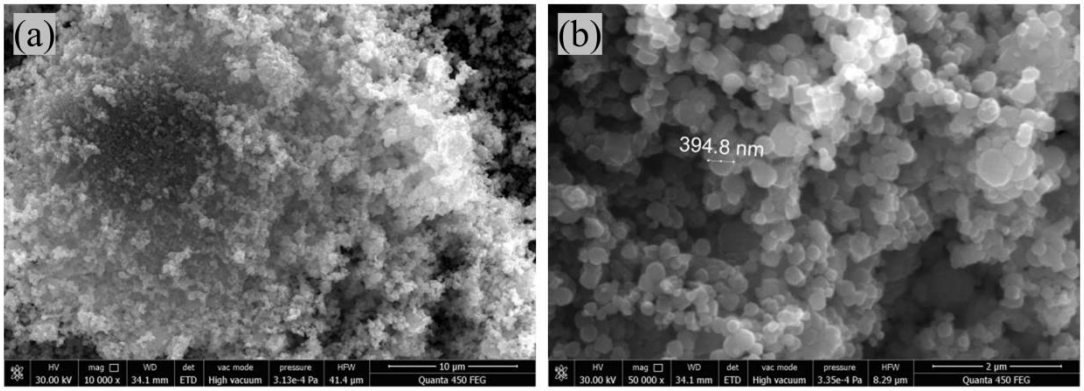

Figure 12. SEM images of Fe_3O_4. (**a**) Magnification 30 K; (**b**) Magnification 50 K.

3.2. Experimental Procedures

Experiments were performed in 250 mL beakers with 100 mL BPA solutions. The required amounts of PS and Fe_3O_4 were added to the solution to start the reaction. At the same time, the solutions were agitated to mix the various substances well. The samples were taken from beaks every 10 min to determine BPA concentrations. Before testing the BPA concentration, the water samples need to be filtered through a 0.45 μm filter membrane and filled with methanol to quench the free radical reaction. The pH of the solution was adjusted using sodium hydroxide and sulfuric acid according to the protocol of the experiment.

3.3. RSM Design

The effect of the interaction of magnetite dosage (A), PS concentration (B), and initial pH (C) on BPA removal was investigated using response surface methodology (RSM) and Design-Expert Software analysis. Following Box-Behnken's method, a total of 17 three-parameter and three-level experiments were designed for BPA removal by the Fe_3O_4/PS system. The composition of the experimental points is shown in Figure 13. There are 12 centroids along the edge lines represented as hollow spheres, and only one cube center is marked with a solid sphere. For the centroids of the edge lines, the coordinates of the independent variables are ±1 in all dimensions, except for the one-dimensional independent variables, which are zero. The three-dimensional coordinates of the cube center are all zero. The experiment is repeated five times for the cube center to eliminate experimental errors. Therefore, a total of 17 sets of experiments are required. The mathematical relationship between response and independent variables could be represented by Equation (2) [38]. In Equation (2), X_i is the coded value of the independent variables; Y is the predicted response value; β_0, β_i, and β_{ii} are the offset, linear offset, and second-order offset terms, respectively; β_{ij} is the interaction coefficient; and k is the number of independent variables.

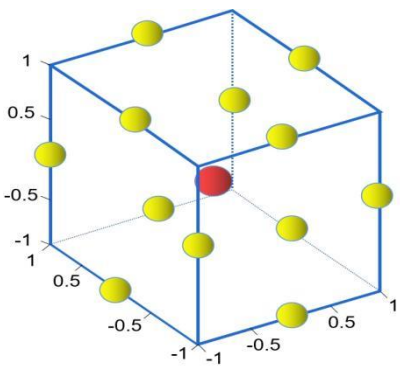

Figure 13. Schematic diagram of three-factor and three-level experiments.

$$Y = \beta_0 + \sum_{i=1}^{k} \beta_i X_i + \sum_{i<j}^{k} \beta_{ij} X_i X_j + \sum_{i=1}^{k} \beta_{ii} X_i^2 \quad (2)$$

3.4. Analysis Methods

High-performance liquid chromatography (G7121A, Agilent, Santa Clara, CA, USA) with a fluorescence detector was used to determine the concentration of BPA in water samples. The instrument was equipped with a C18 column (4.6 mm × 150 mm, 4 μm). The mobile phase was methanol and water with a volume ratio of 70:30. The injection volume was 20 μL and the flow rate was 0.8 mL/min. The column temperature was 25 °C. The excitation and emission wavelengths were 228 nm and 312 nm, respectively.

The BPA removal rate was obtained from Equation (3). In this equation, C_0 (mg/L) and C_t (mg/L) are the initial BPA concentration and the concentration at moment t, respectively.

$$BPAremoval\ (\%) = \frac{(C_0 - C_t)}{C_0} \times 100\% \quad (3)$$

4. Conclusions

The effect of four factors on BPA degradation was examined in the system Fe_3O_4/PS. Three important influencing factors—magnetite dosage, PS concentration, and pH—were selected for response surface optimization experiments.

The experimental conditions of the Fe_3O_4/PS degradation of BPA were optimized using the Box-Behnken response surface methodology. The quadratic polynomial regression equation established with the BPA degradation rate as the response value was highly significant: p-value < 0.05, R^2 was 0. 9152, the misfit term was not significant, and the regression equation fit well with the actual situation.

The interaction between the three influencing factors was optimized by the response surface methodology, and the optimal conditions for the degradation of BPA in Fe_3O_4/PS were obtained by Design-Expert software as follows: 0.3 g/L of magnetite, 0.26 mM of PS, and pH 4.9. Under these conditions, the BPA degradation rate was 59.54%, which was close to the real value of 65.52% (0.3 g/L of magnetite, 0.3 mM of PS, pH 5.0). It was verified that the experimental values were close to the model predictions, indicating that the equations were well fitted and the best response conditions were reliable.

Author Contributions: Conceptualization, methodology, software, and validation, S.C.; formal analysis, investigation, and data curation, Y.Y.; writing—original draft preparation, writing—review and editing, and visualization, S.C.; supervision and project administration, Y.Y. All authors have read and agreed to the published version of the manuscript.

Funding: This research received no external funding.

Data Availability Statement: No new data were created or analyzed in this study. Data sharing is not applicable to this article.

Conflicts of Interest: The authors declare no conflict of interest.

References

1. Godswill, A.C.; Godspel, A.C. Physiological effects of plastic wastes on the endocrine system (Bisphenol A, Phthalates, Bisphenol S, PBDEs, TBBPA). *Int. J. Bioinform. Comput. Biol.* **2019**, *4*, 11–29.
2. Wnuczek, K.; Puszka, A.; Podkościelna, B. Synthesis and spectroscopic snalyses of new polycarbonates based on bisphenol A-free components. *Polymers* **2021**, *13*, 4437. [CrossRef]
3. Tijani, J.O.; Fatoba, O.O.; Petrik, L.F. A review of pharmaceuticals and endocrine-disrupting compounds: Sources, effects, removal, and detections. *Water Air Soil Pollut.* **2013**, *224*, 1170. [CrossRef]
4. Ma, D.; Yi, H.; Lai, C.; Liu, X.; Huo, X.; An, Z.; Li, L.; Fu, Y.; Li, B.; Zhang, M.; et al. Critical review of advanced oxidation processes in organic wastewater treatment. *Chemosphere* **2021**, *275*, 130104. [CrossRef] [PubMed]
5. Umar, M.; Roddick, F.; Fan, L.; Aziz, H.A. Application of ozone for the removal of bisphenol A from water and wastewater—A review. *Chemosphere* **2013**, *90*, 2197–2207. [CrossRef] [PubMed]

6. Diao, Z.-H.; Dong, F.-X.; Yan, L.; Chen, Z.-L.; Qian, W.; Kong, L.-J.; Zhang, Z.-W.; Zhang, T.; Tao, X.-Q.; Du, J.-J.; et al. Synergistic oxidation of Bisphenol A in a heterogeneous ultrasound-enhanced sludge biochar catalyst/persulfate process: Reactivity and mechanism. *J. Hazard. Mater.* **2020**, *384*, 121385. [CrossRef] [PubMed]
7. Kong, L.; Fang, G.; Chen, Y.; Xie, M.; Zhu, F.; Ma, L.; Zhou, D.; Zhan, J. Efficient activation of persulfate decomposition by Cu2FeSnS4 nanomaterial for bisphenol A degradation: Kinetics, performance and mechanism studies. *Appl. Catal. B Environ.* **2019**, *253*, 278–285. [CrossRef]
8. Deng, Y.; Zhao, R. Advanced Oxidation Processes (AOPs) in Wastewater Treatment. *Curr. Pollut. Rep.* **2015**, *1*, 167–176. [CrossRef]
9. Oh, W.-D.; Dong, Z.; Lim, T.-T. Generation of sulfate radical through heterogeneous catalysis for organic contaminants removal: Current development, challenges and prospects. *Appl. Catal. B Environ.* **2016**, *194*, 169–201. [CrossRef]
10. Akbari, S.; Ghanbari, F.; Moradi, M. Bisphenol A degradation in aqueous solutions by electrogenerated ferrous ion activated ozone, hydrogen peroxide and persulfate: Applying low current density for oxidation mechanism. *Chem. Eng. J.* **2016**, *294*, 298–307. [CrossRef]
11. Bose, S.; Kumar, M. Microwave-assisted persulfate/peroxymonosulfate process for environmental remediation. *Curr. Opin. Chem. Eng.* **2022**, *36*, 100826. [CrossRef]
12. Wang, J.; Wang, S. Activation of persulfate (PS) and peroxymonosulfate (PMS) and application for the degradation of emerging contaminants. *Chem. Eng. J.* **2018**, *334*, 1502–1517. [CrossRef]
13. Fedorov, K.; Plata-Gryl, M.; Khan, J.A.; Boczkaj, G. Ultrasound-assisted heterogeneous activation of persulfate and peroxymonosulfate by asphaltenes for the degradation of BTEX in water. *J. Hazard. Mater.* **2020**, *397*, 122804. [CrossRef] [PubMed]
14. Ahmadi, M.; Ghanbari, F.; Moradi, M. Photocatalysis assisted by peroxymonosulfate and persulfate for benzotriazole degradation: Effect of pH on sulfate and hydroxyl radicals. *Water Sci. Technol.* **2015**, *72*, 2095–2102. [CrossRef] [PubMed]
15. Forouzesh, M.; Ebadi, A.; Aghaeinejad-Meybodi, A. Degradation of metronidazole antibiotic in aqueous medium using activated carbon as a persulfate activator. *Sep. Purif. Technol.* **2018**, *210*, 145–151. [CrossRef]
16. Li, L.; Zhang, Y.; Yang, S.; Zhang, S.; Xu, Q.; Chen, P.; Du, Y.; Xing, Y. Cobalt-loaded cherry core biochar composite as an effective heterogeneous persulfate catalyst for bisphenol A degradation. *RSC Adv.* **2022**, *12*, 7284–7294. [CrossRef]
17. Zhang, B.-T.; Zhang, Y.; Teng, Y.; Fan, M. Sulfate radical and its application in decontamination technologies. *Crit. Rev. Environ. Sci. Technol.* **2014**, *45*, 1756–1800. [CrossRef]
18. Gao, Y.; Champagne, P.; Blair, D.; He, O.; Song, T. Activated persulfate by iron-based materials used for refractory organics degradation: A review. *Water Sci. Technol.* **2020**, *81*, 853–875. [CrossRef]
19. Gao, F.; Li, Y.; Xiang, B. Degradation of bisphenol A through transition metals activating persulfate process. *Ecotoxicol. Environ. Saf.* **2018**, *158*, 239–247. [CrossRef]
20. Jiang, X.; Wu, Y.; Wang, P.; Li, H.; Dong, W. Degradation of bisphenol A in aqueous solution by persulfate activated with ferrous ion. *Environ. Sci. Pollut. Res.* **2013**, *20*, 4947–4953. [CrossRef]
21. dos Santos, A.J.; Sirés, I.; Brillas, E. Removal of bisphenol A from acidic sulfate medium and urban wastewater using persulfate activated with electroregenerated Fe^{2+}. *Chemosphere* **2021**, *263*, 128271. [CrossRef] [PubMed]
22. Zhao, L.; Ji, Y.; Kong, D.; Lu, J.; Zhou, Q.; Yin, X. Simultaneous removal of bisphenol A and phosphate in zero-valent iron activated persulfate oxidation process. *Chem. Eng. J.* **2016**, *303*, 458–466. [CrossRef]
23. Girit, B.; Dursun, D.; Olmez-Hanci, T.; Arslan-Alaton, I. Treatment of aqueous bisphenol A using nano-sized zero-valent iron in the presence of hydrogen peroxide and persulfate oxidants. *Water Sci. Technol.* **2015**, *71*, 1859–1868. [CrossRef] [PubMed]
24. Dong, Z.; Zhang, Q.; Chen, B.Y.; Hong, J. Oxidation of bisphenol A by persulfate via Fe_3O_4-α-MnO_2 nanoflower-like catalyst: Mechanism and efficiency. *Chem. Eng. J.* **2019**, *357*, 337–347. [CrossRef]
25. Ioffe, M.; Long, M.; Radian, A. Systematic evaluation of activated carbon-Fe_3O_4 composites for removing and degrading emerging organic pollutants. *Environ. Res.* **2021**, *198*, 111187. [CrossRef]
26. Zhu, Y.; Yue, M.; Natarajan, V.; Kong, L.; Ma, L.; Zhang, Y.; Zhao, Q.; Zhan, J. Efficient activation of persulfate by Fe_3O_4@β-cyclodextrin nanocomposite for removal of bisphenol A. *RSC Adv.* **2018**, *8*, 14879–14887. [CrossRef]
27. Safabakhsh, T.; Daraei, H.; Saha, N.; Khodakarim, S. Degradation of Bisphenol A from aqueous solutions using Fe_3O_4 as a persulfate activator. *Desalin. Water Treat.* **2019**, *166*, 115–121. [CrossRef]
28. Rao, Y.; Qu, L.; Yang, H.; Chu, W. Degradation of carbamazepine by Fe(II)-activated persulfate process. *J. Hazard. Mater.* **2014**, *268*, 23–32. [CrossRef]
29. Zhao, Y.S.; Sun, C.; Sun, J.Q.; Zhou, R. Kinetic modeling and efficiency of sulfate radical-based oxidation to remove p-nitroaniline from wastewater by persulfate/Fe_3O_4 nanoparticles process. *Sep. Purif. Technol.* **2015**, *142*, 182–188. [CrossRef]
30. Wei, Y.; Han, B.; Hu, X.; Lin, Y.; Wang, X.; Deng, X. Synthesis of Fe_3O_4 Nanoparticles and their Magnetic Properties. *Procedia Eng.* **2012**, *27*, 632–637. [CrossRef]
31. Zhu, C.; Fang, G.; Dionysiou, D.D.; Liu, C.; Gao, J.; Qin, W.; Zhou, D. Efficient transformation of DDTs with persulfate activation by zero-valent iron nanoparticles: A mechanistic study. *J. Hazard. Mater.* **2016**, *316*, 232–241. [CrossRef]
32. Zhang, Y.Q.; Du, X.Z.; Huang, W.L. Temperature effect on the kinetics of persulfate oxidation of p-chloroaniline. *Chin. Chem. Lett.* **2011**, *22*, 358–361. [CrossRef]
33. He, W.; Zhu, Y.; Zeng, G.; Zhang, Y.; Wang, Y.; Zhang, M.; Long, H.; Tang, W. Efficient removal of perfluorooctanoic acid by persulfate advanced oxidative degradation: Inherent roles of iron-porphyrin and persistent free radicals. *Chem. Eng. J.* **2019**, *392*, 123640. [CrossRef]

34. Tunç, M.S. Decolorization of azo dye Everdirect Supra Red BWS in an aqueous solution by heat-activated persulfate: Optimization using response surface methodology. *Desalin. Water Treat.* **2019**, *158*, 372–384. [CrossRef]
35. Yuan, D.; Zhang, C.; Tang, S.; Sun, M.; Zhang, Y.; Rao, Y.; Wang, Z.; Ke, J. Fe^{3+}-sulfite complexation enhanced persulfate Fenton-like process for antibiotic degradation based on response surface optimization. *Sci. Total Environ.* **2020**, *727*, 138773. [CrossRef] [PubMed]
36. Kusic, H.; Peternel, I.; Koprivanac, N.; Bozic, A.L. Iron-activated persulfate oxidation of an azo dye in model wastewater: Influence of iron activator type on process optimization. *J. Environ. Eng.* **2011**, *137*, 454–463. [CrossRef]
37. Han, Y.; Zhou, X.; Lei, L.; Sun, H.; Niu, Z.; Zhou, Z.; Xu, Z.; Hou, H. Efficient activation of persulfate by calcium sulfate whisker supported nanoscale zero-valent iron for methyl orange removal. *RSC Adv.* **2021**, *11*, 452–461. [CrossRef]
38. Silveira, J.E.; Barreto-Rodrigues, M.; Cardoso, T.O.; Pliego, G.; Munoz, M.; Zazo, J.A.; Casas, J.A. Nanoscale Fe/Ag particles activated persulfate: Optimization using response surface methodology. *Water Sci. Technol.* **2017**, *75*, 2216–2224. [CrossRef]